

On-Flow Immobilization of Polystyrene Microspheres on β -Cyclodextrin-Patterned Silica Surfaces through Supramolecular Host–Guest Interactions

Stan B.J. Willems,^{†,‡,§} Anton Bunschoten,^{†,‡} R. Martijn Wagterveld,[§] Fijis W.B. van Leeuwen,^{†,‡} and Aldrik H. Velders^{*,†,‡,§}

[†]Laboratory of BioNanoTechnology, Wageningen University and Research, Axis, Bornse Weiland 9, 6708 WG Wageningen, The Netherlands

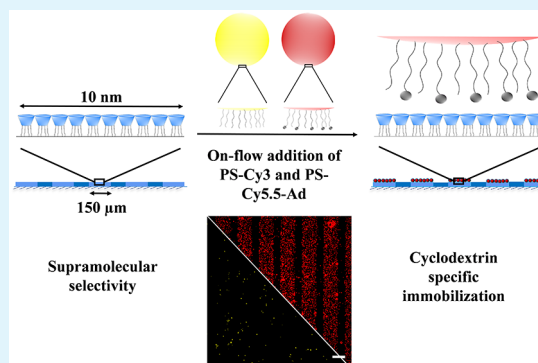
[‡]Interventional Molecular Imaging Laboratory, Department of Radiology, Leiden University Medical Center, Albinusdreef 2, 2333 ZA Leiden, The Netherlands

[§]Wetsus, European Centre of Excellence for Sustainable Water Technology, Oostergoweg 9, 8911 MA Leeuwarden, The Netherlands

Supporting Information

ABSTRACT: Species-specific isolation of microsized entities such as microplastics and resistant bacteria from waste streams is becoming a growing environmental challenge. By studying the on-flow immobilization of micron-sized polystyrene particles onto functionalized silica surfaces, we ascertain if supramolecular host–guest chemistry in aqueous solutions can provide an alternative technology for water purification. Polystyrene particles were modified with different degrees of adamantane (guest) molecules, and silica surfaces were patterned with β -cyclodextrin (β -CD, host) through microcontact printing (μ CP). The latter was exposed to solutions of these particles flowing at different speeds, allowing us to study the effect of flow rate and multivalency on particle binding to the surface. The obtained binding profile was correlated with Comsol simulations. We also observed that particle binding is directly aligned with particle's ability to form host–guest interactions with the β -CD-patterned surface, as particle binding to the functionalized glass surface increased with higher adamantane load on the polystyrene particle surface. Because of the noncovalent character of these interactions, immobilization is reversible and modified β -CD surfaces can be recycled, which provides a positive outlook for their incorporation in water purification systems.

KEYWORDS: microparticles, flow cell, water purification, microcontact printing, supramolecular chemistry



1. INTRODUCTION

Studying the interactions of microparticles with chemically modified surfaces is an important step in the development of cell-targeting platforms.^{1,2} Immobilization of cells, for instance, bacteria, to monolayers on surfaces provides an interesting field of research, especially toward medical or water treatment applications.^{3–6} However, within complex biological systems, such as bacterial cells, it is difficult to investigate specific surface adhesion interactions of microsized entities with functionalized surfaces. Importantly, the feasibility of particle adhesion interactions with respect to different length scales being studied, that is, between microparticles and molecules, should be confirmed using a more controllable model system. Therefore, the use of model microparticles such as polystyrene (PS) particles, which have the same size as most bacteria, is a versatile and valuable tool for investigating adhesion onto chemically functionalized surfaces.

In nature, the binding mechanisms of microsized entities such as cells are governed by numerous amounts of interactions. Among these interactions, hydrophobicity plays a significant role in the attachment or detachment of cells to surfaces.⁷ Therefore, Whitesides et al. have carried out protein and cell adhesion studies by using monolayers of alkanethiols or alkylsilanes on gold or silicon surfaces in order to mimic cell-binding mechanisms within nature.^{8–11} Patterning of the surfaces through a soft lithographic technique, such as microcontact printing (μ CP),^{12,13} allowed for spatial control of cell adhesion, which improved confirmation of binding during analysis. In order to acquire more specificity within cell adhesion studies, different targeting agents for bacteria were

Received: June 24, 2019

Accepted: September 5, 2019

Published: September 5, 2019

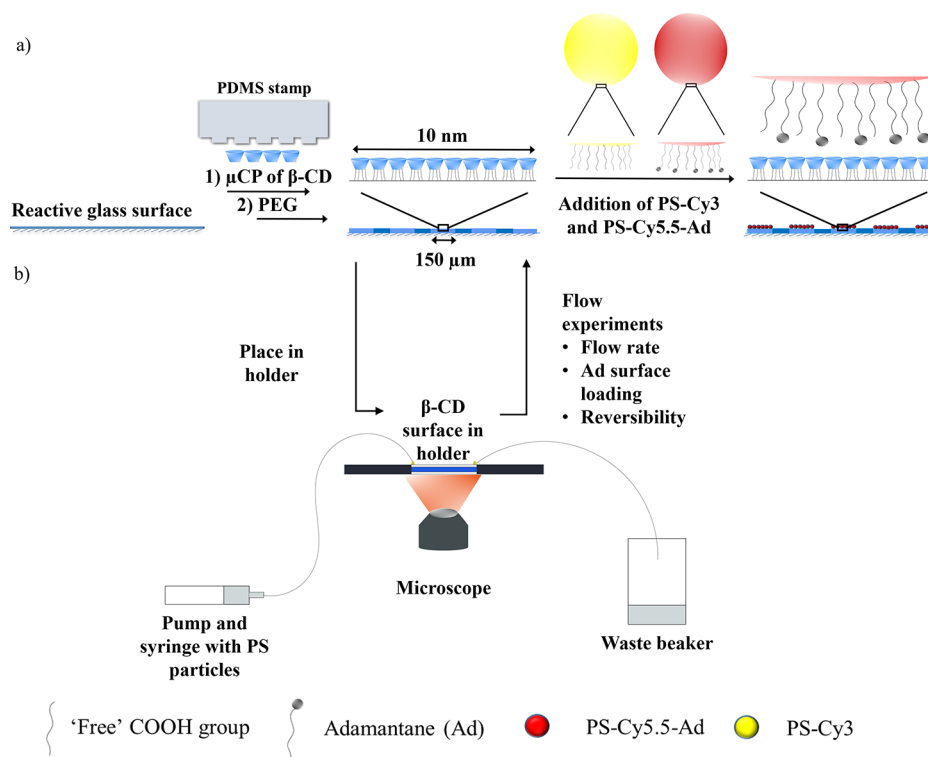


Figure 1. (a) Scheme showing μ CP of β -CD on the glass surface and backfilling with poly(ethylene glycol) (PEG) and the principle of binding: combined addition of nonfunctionalized PS particles with Cyanine 3 (Cy3) fluorescent label (PS-Cy3, negative control) and Ad-functionalized PS particles with Cyanine 5.5 (Cy5.5) fluorescent label (PS-Cy5.5-Ad) to patterned β -CD surfaces. (b) Flow cell holder setup on a fluorescence microscope containing a functionalized glass surface to perform different types of flow experiments.

investigated by Sankaran et al., who adhered bacteria to surfaces via an azobenzene–mannose linker and a trans-membrane protein containing tryptophan and phenylalanine on cucurbit[8]uril layers.^{14,15} Moreover, Di Iorio et al. studied the binding kinetics of virus mimics to sialic acid residues via weak multivalent interactions in order to predict the number of interactions involved in binding.¹⁶ Based on these advances, the implementation and investigation of supramolecular and multivalent interactions for high-affinity, noncovalent, and reversible binding is an important aspect for understanding cell immobilization. We here exploit this type of binding as an outlook toward water treatment applications, as it is desirable to capture cells rapidly and subsequently release immobilized cells for reusability of surfaces.

For fabrication of reusable surfaces, we selected the noncovalent binding of adamantane (Ad) to β -cyclodextrin (β -CD). Cyclodextrins are cyclic carbohydrate molecules consisting of 1,4- α -D-glucopyranosides bound in a cone shape¹⁷ and are used primarily in food, pharmaceutical, and drug-delivery applications.^{18,19} Hydrophobic molecules can form reversible inclusion complexes through hydrophobic and van der Waals interactions (host–guest chemistry) with the cyclodextrin cavity. Tethering of β -CD on silicon dioxide surfaces,²⁰ known as the molecular printboard,²¹ has been carried out by Reinhoudt and co-workers. This led to binding control and characterizing binding strength of functionalized dendrimers, nanoparticles, and fluorescent guest molecules with cyclodextrin inside their hydrophobic cavity. In later work by Gonzalez-Campo et al., patterns of β -CD were created on glass surfaces through reactive μ CP, showcasing the possibility of fluorescent guest adsorption from the solution to β -CD patterns or orthogonal supramolecular printing of fluorescent

guests.²² The fluorescent guest molecules in these cases contain two Ad moieties, which have a high affinity for the β -CD cavity in water.²³ Furthermore, the reversibility and reusability of this system has been tested by forming multivalent networks of β -CD-modified gold nanoparticles with diferrocene-modified peptides, which functioned as an ultrasensitive enzyme sensor.²⁴ In order to test the immobilization via host–guest interactions with larger constructs than molecules, silica nanoparticles and quantum dots have also been immobilized on β -CD surfaces using an intermediary Ad-functionalized dendrimer as “glue”.^{25,26} The high binding affinity of multivalent host–guest interactions has also been used for the adhesion of macroscopic acrylamide gels.²⁷ Based on these examples, the versatility of host–guest interactions mediated by β -CD provides a reliable tool for scaling up from nanoparticles to specific and reversible immobilization of microparticles.

To study the supramolecular adhesion of microparticles, we functionalized PS particles with different amounts of Ad on their surface, patterned glass surfaces with β -CD, and subsequently applied a flow of functionalized particles over the modified glass surface (Figure 1a). PEG backfilling is included as an antifouling layer between β -CD patterns. The functionalized glass slides were placed in a holder which was connected to a syringe pump for controlling the flow rate of PS particle solutions over the glass slides. Host–guest interactions between β -CD and Ad allow for the capture of the functionalized PS particles on the glass surface, which can then be analyzed via fluorescence microscopy. Figure 1b shows how the flow cell holder setup is directly incorporated on the microscope to carry out various flow experiments for characterizing binding of PS particles to the β -CD-function-

alized glass slide. Results regarding the feasibility of this approach can also be used as a proof-of-concept for the application in immobilizing similar-sized cells such as bacteria.

2. EXPERIMENTAL SECTION

2.1. Synthesis and Functionalization of Fluorescent PS Particles. PS particles (10 wt %, $\sim 1 \mu\text{m}$) were synthesized following the protocol from Appel et al. using the reaction mixture “pSIA25”.²⁸ Then, 125 g of deionized (DI) water, 25 g of styrene, 0.5 g of itaconic acid, and 0.01 g of the fluorescent dye Cy3 or Cy5.5 (used for staining the core of resulting PS particles, as shown in Figure S1) were taken in a one-neck round-bottom flask. The flask was sealed with a rubber septum, and the reaction mixture was flushed with nitrogen for 15 min, followed by heating at 85 °C and stirring at 500 rpm for 15 min. A 0.1 M solution of 4,4'-azobis(4-cyanovaleric acid) was prepared in 0.2 M NaOH, and 8.92 mL (0.25 g) of this solution was injected to the reaction mixture to initiate colloid synthesis. The reaction was allowed to proceed for at least 12 h at 85 °C and stirring at 500 rpm. The following day, the reaction mixture was filtered, spun down through centrifugation at 3260g for 30 min, and then washed three times with DI water through centrifugation at 3260g for 30 min per washing step. The concentration in wt % was determined through freeze-drying PS particles and then measuring the mass of the lyophilized particles. A 5 mL solution of 0.5% wt of PS-Cy5.5 particles in 10 mM 2-(*N*-morpholino)ethanesulfonic acid buffer, pH 5.0, was modified with 0.53, 1.33, and 2.67 μmol of 1-adamantylamine hydrochloride using 0.32 mmol 1-ethyl-3-(3-dimethylaminopropyl)-carbodiimide hydrochloride (EDC), according to the covalent coupling protocol from Bangs Laboratories, Inc.²⁹ After overnight EDC coupling, the dispersion of PS particles was spun down in a centrifuge at 3260g (30 min) and subsequently washed three times with DI water also by centrifugation at 3260g (30 min per washing step) in order to remove nonreacted 1-adamantylamine.

2.2. Dynamic Light Scattering (DLS) Measurements. Dispersions of PS particle samples were diluted to an appropriate concentration with DI water and then analyzed on a Malvern Zetasizer Nano S using the size intensity values. The samples were measured three times with 10 runs per measurement at 25 °C. The size of all particles was determined to be ca. 1 μm (Figure S2).

2.3. Conductometric Titration. As-synthesized fluorescent PS-Cy5.5 particles were diluted 40 \times in 20 mL of DI water. The pH was adjusted to 10 by using 10 mM NaOH to deprotonate all the carboxyl groups on the PS particle surface. The conductivity of the dispersion of PS particles was then measured upon addition of 2 mM HCl in 40 μL increments until ca. pH 4.5 was reached. The data were plotted as volume 2 mM HCl added versus conductivity of the PS solution. From this graph, the total amount of CO₂H groups on the PS particle surface could be determined.³⁰

2.4. ¹H NMR Spectroscopy. The supernatant of PS particles after EDC coupling with 1-adamantylamine hydrochloride was collected and concentrated by rotary evaporation. The resulting product was resuspended in 1 mL of deuterated water (D₂O) with 1 mM trimethylsilylpropionic acid (TMSP) as the internal standard. A Bruker 500 MHz NMR system was used for obtaining the ¹H NMR spectra. The characteristic Ad peaks at 1.6 ppm in supernatant samples were integrated to the TMSP peak at 0 ppm to calculate the concentration of unreacted Ad left in each sample. Ad left within the dispersion of PS particles could then be determined by the difference between the Ad added to the reaction mixture compared to the unreacted Ad left in the supernatant.

2.5. Glass Surface Functionalization. Isothiocyanate monolayers on glass were prepared as described by Onclin et al.,²⁰ and the glass slides were cleaned and oxidized with piranha solution (H₂SO₄ (95–98%)/H₂O₂ (35%), 3:1 v/v; *Warning! Piranha solutions must be handled with caution as they may unexpectedly detonate*) for 45 min, rinsed with large amounts of DI water, and dried under a N₂ atmosphere. The glass slides were placed in a high vacuum preheated desiccator together with a glass vial containing 1 mL of 3-aminopropyltriethoxysilane (APTES, 99%) and then in an oven at

70 °C overnight. Following amine monolayer formation, the glass slides were removed from the desiccator and rinsed with toluene and dichloromethane. The glass slides were then cured for at least 1 h in the oven at 70 °C. Next, the glass slides were immersed in 0.1 M 1,4-phenylene diisothiocyanate (PDITC) in anhydrous toluene for 2 h under an argon atmosphere to yield isothiocyanate-bearing layers. Following immersion, the surfaces were rinsed with toluene and dichloromethane and used immediately for μCP . Stamps were made by using a technique reported by Whitesides.¹⁰ Then, the stamps were prepared by casting a 10:1 (w/w) mixture of poly(dimethylsiloxane) (PDMS) and a curing agent (Sylgard 184, Dow Corning) onto a silicon master to yield PDMS stamps with 150 μm broad line patterns and 50 μm broad spacing between the lines. After overnight curing at 70 °C, the PDMS stamps were cut out, oxidized by high-energy air plasma for 1 min, and incubated in 0.72 mM heptakis(6-amino-6-deoxy)- β -CD heptahydrochloride aqueous solution, pH 8.0, for 2 h. Before printing, excess solution was dried off from the stamp surfaces using a stream of nitrogen. The PDMS stamps were then brought into conformal contact with the freshly prepared isothiocyanate-functionalized glass surfaces for 30 min. After carefully removing the stamps, the printed glass substrates were rinsed thoroughly with DI water. The glass substrates were then incubated overnight in 1 mM methoxy PEG amine (PEG-NH₂, *M*_w 2000 Da, Iris Biotech GmbH) aqueous backfilling solution, pH 8.0, to react with unreacted isothiocyanates. Before use, the glass substrates were rinsed with DI water. When not used within a day, substrates were stored in the backfilling solution at 4 °C.

2.6. Validation of β -CD Patterns. The β -CD-printed glass substrates were incubated for 15 min on a droplet of 0.28 μM Cy5.5 dye solution in phosphate-buffered saline (PBS), functionalized with two adamantyl moieties (Cy5-Ad₂,³¹ structures shown in Figure S1). After removal of the glass substrates from the solution, they were rinsed with DI water and dried with nitrogen. The substrates were then analyzed by fluorescence microscopy.

2.7. Flow Experiments. An equimolar mixture of PS-Cy3 and PS-Cy5.5-Ad at pH ≈ 10 was made to flow through a resealable flow cell holder (fluidic connect PRO Resealable, Micronit; for dimensions see Figure S3a + b) containing a β -CD-printed glass surface (4515 extended resealable flow cells, Micronit) using a syringe pump. The pH of the PS particles was increased to 10 using 0.1 M NaOH to ensure that unreacted amine groups of heptakis(6-amino-6-deoxy)- β -CD on the glass surface were not protonated and therefore remain uncharged. Flow rates and pumping times of 0.125 (40 h), 0.25 (20 h), 1.25 (4 h), 2.5 (2 h), 5 (1 h), 10 (30 min), 100 (3 min), and 200 (1.5 min) $\mu\text{L}/\text{min}$ were used to pump the particle solution over the glass surfaces. The pumping time, listed in brackets after the respective flow rate, was adjusted for different flow rates to keep the same total amount of PS particles flowing over the surface. The flow cell holder was placed directly on the stage of a Leica DMI8 epifluorescence microscope to allow imaging before, during, and after flow. After flow incubation, the pump was switched off and the inlet tubing was removed, causing the solution to flow out of the resealable flow cell through the capillary effect.

2.8. Calculating Particle Density and Binding Specificity of Particles. The particle density on β -CD patterns was determined through analysis of microscope images after flow experiments. For acquiring an average particle density, all individual experiments were carried out three times and per glass slide the start, middle, and the end of the flow path were analyzed using ImageJ software (9 images in total). The pixels related to nonaggregated particles were initially segmented out of the image using the “Analyze particles” function. Subsequently, the average pixel size for one particle was determined. With the “Measure” function, the pixels were counted over the desired line patterns (on β -CD patterns or PEG backfilling), which were then converted into amounts of particles based on the determined average pixel size for one particle. The particle density over 100 μm^2 was subsequently calculated based on the total surface area of desired line patterns (β -CD or PEG patterns) per image. The binding specificity of particles for β -CD-printed patterns was then calculated as a percentage with the following formula

$$\eta = \frac{\sigma_p}{\sigma_p + \sigma_n} \times 100$$

Here, η (%) is the binding specificity, σ_p (μm^{-2}) is the particle density on the β -CD patterns, and σ_n (μm^{-2}) is the particle density on the PEG spacing. Throughout the results and discussion, the terms “specificity” and “selectivity” will be used frequently. Specificity is a comparison between binding of PS-Cy5.5-Ad to either β -CD or PEG while selectivity is a comparison between PS-Cy5.5-Ad or PS-Cy3 binding to β -CD.

2.9. Comsol Simulations. For simulating the flow experiments, Comsol Multiphysics 5.4 with the Particle Tracing Module was used. A 2D design of the microchannel was made (20×0.3 mm, similar to the extended channel part of the Micronit resealable flow cell) with an inlet on the left, outlet on the right, and stick conditions for the top and the bottom channel wall (Figure S3c). For the simulations, particles of 1 μm were chosen and the following conditions were applied: gravity, Brownian motion, and creeping/laminar flow conditions. To simulate the different flow rates used, the average flow velocity and particle release times were varied between 0.0625 and 200 $\mu\text{L}/\text{min}$ (shown in Table 1). The particle addition time

Table 1. Table Showing Conversion of Flow Rate to Average Flow Velocity and the Particle Addition Times for Different Flow velocities^a

flow rate ($\mu\text{L min}^{-1}$)	average flow velocity within the flow channel (m s^{-1})	particle addition times (start, interval, end) (s)
0.0625	2.14×10^{-7}	0, 8000, 288 000
0.125	5.35×10^{-7}	0, 4000, 144 000
0.25	1.07×10^{-6}	0, 2000, 72 000
1.25	5.35×10^{-6}	0, 400, 14 400
2.5	1.07×10^{-5}	0, 200, 7200
5	2.14×10^{-5}	0, 100, 3600
10	4.27×10^{-5}	0, 50, 1800
100	4.27×10^{-4}	0, 5, 180
200	8.54×10^{-4}	0, 2.5, 90

^a40 particles are added at time 0 s and at the given intervals with a total of 1480 particles for each simulation.

entails the specific time points at which particles were infused into the designed channel and are given as the start time (in all cases at time 0 s), the interval time between the start and the end time (i.e., if 200 s, every 200 s, 40 particles are added), and the end time of the simulation for which no particles are added.

3. RESULTS AND DISCUSSION

Patterned monolayers of β -CD were fabricated on glass surfaces, and Ad-functionalized fluorescent PS microparticles were synthesized with different degrees of Ad-surface loading, ranging from 0.15 to 0.8 Ad mole fraction of the available CO_2H groups on the PS particle surface. Both the surface functionalization and synthesis of modified particles were characterized. Then, the immobilization of the particles on the glass surface in flow, via host–guest interactions, was validated through patterned binding of particles. For reference, a control PS particle without Ad functionality was always included to check the selectivity of the system. Various flow experiments were carried out to further investigate this model system, namely, flow rate variation, immobilization of PS particles with different Ad loading on the PS surface, and reusability of the glass slides after removal of bound PS particles.

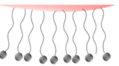
3.1. Characterization. **3.1.1. Fabrication of β -CD Patterns through μCP .** Glass slides were first silanized with APTES and then functionalized with 1,4-phenylene diisothiocyanate (PDITC) to create a surface reactive toward amines.

The patterning of isothiocyanate glass slides with heptakis amino β -CD was achieved through μCP ,¹³ and the unreacted areas were filled with PEG-NH₂ (the first step in Figure 1b). Patterning was performed using μCP functions as an internal control to observe the specific assembly of molecules or particles on the β -CD surface. According to the literature,^{20,32} the presence of β -CD patterns on the surface can be validated through the addition of diadamantane-functionalized fluorophores. We used a Cy5.5 (Cy5-Ad₂) functionalized with two Ad molecules for detecting β -CD patterns on the surface, which yielded a bright fluorescence signal over printed lines of β -CD (Figure S4). Rinsing with DI water did not remove bound Cy5-Ad₂, which indicates the presence of a high affinity interaction between Cy5-Ad₂ and β -CD.

3.1.2. PS Particle Characterization and Functionalization with Ad Amine. PS particles covered with carboxyl groups were synthesized according to the protocol demonstrated by Appel et al.,²⁸ with either Cy3 or Cy5.5 (Figure S1) dye used to stain the PS cores. This allowed for facile analysis and discrimination using fluorescence imaging. After particle synthesis, the concentration of PS particles was determined: a known volume of the particles was lyophilized and the resulting particles were weighed to determine the mass concentration (Table S1). From this value, we calculated the as-synthesized particles to have a concentration of 1.82×10^{11} PS particles/mL (eq S1). The amount of CO_2H groups per PS particle was then determined at 2.4×10^7 through reverse conductometric titration (Figure S5).³⁰

PS-Cy5.5 particles were modified with 0.53, 1.33, and 2.67 μmol of Ad amine via an EDC coupling reaction. Ad surface loading on PS particles was determined through ¹H NMR spectroscopy of the PS particle supernatant (Figures S6 and S7), and the PS particle samples were named after their degree of surface functionalization: PS-Cy5.5-0.15Ad, PS-Cy5.5-0.3Ad, and PS-Cy5.5-0.8Ad (Table 2). However, for PS-

Table 2. Determining the Degree of Surface Functionalization After NMR Analysis of the Supernatant of Different PS-Cy5.5-Ad Samples

PS-Cy5.5-Ad samples			
Ad-NH ₂ added to PS (μmol)	0.53	1.33	2.67
Ad-NH ₂ amount in supernatant (μmol)	0.24	0.70	1.15
Ad-NH ₂ on PS particles (μmol)	0.29	0.63	1.52
Amount of Ad molecules on PS particle	3.9×10^6	8.3×10^6	2×10^7
Ad molecule(s) per nm ² of PS particle surface	~1	~2	~6
Degree of surface functionalization/mole fraction	0.15	0.3	0.8

Cy5.5-0.8Ad, surprisingly high PS surface loading of six Ad molecules per nm² was determined, which is unlikely to reflect six Ad moieties in a densely packed 2D-surface configuration because the effective size of Ad is ca. 0.41 nm² (based on the reported Ad radius of 0.36 nm).³³ This can be explained by the surface roughness of PS particles which increases the total surface area compared to that of the model of a smooth sphere used for carrying out all the calculations.³⁴ The high values for Ad surface loading can also be explained by nonspecific uptake

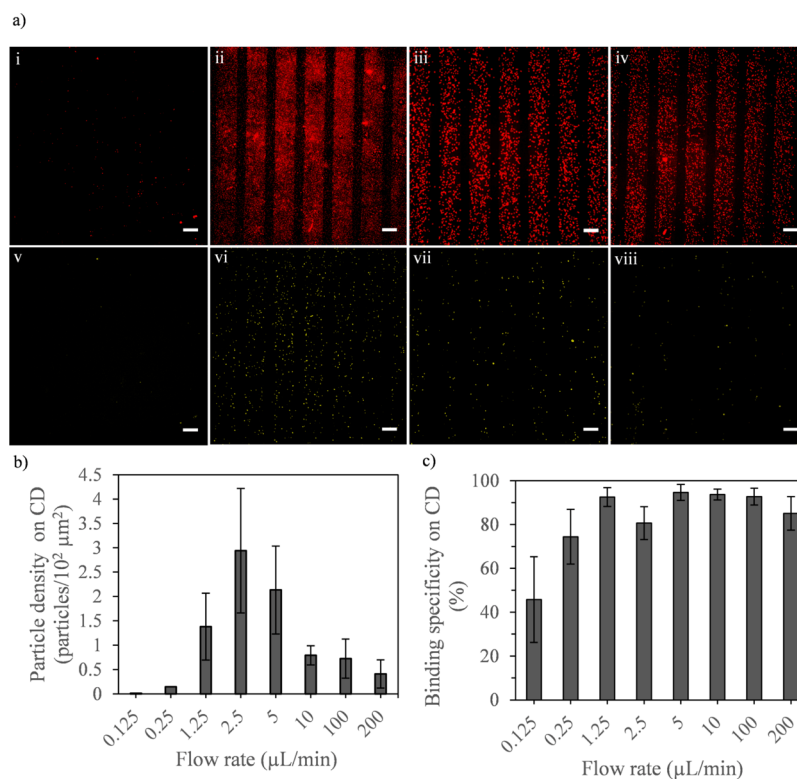


Figure 2. (a) Fluorescence images of patterned β -CD glass surfaces after addition of an equimolar mix of fluorescent PS particles PS-Cy5.5-Ad (i–iv) and PS-Cy3 (v–viii). The patterns are oriented perpendicular to the flow direction. From the left to right, a selection of flow rates are shown: 0.125 (i,v), 2.5 (ii,vi), 100 (iii,vii), and 200 (iv,viii) $\mu\text{L}/\text{min}$. All flow rate experiments are shown in Figure S9. The top images (red) are captured with a Cy5 filter and the bottom images (yellow) with a RHOD filter. Images of different filters and the same flow rate are captured at the same location to compare the effect of aspecific interactions. Scale bars are 100 μm . (b) Graph showing the PS-Cy5.5-Ad particle density on β -CD patterns vs all flow rates used. (c) Graph showing the binding specificity for these respective patterns vs the flow rate.

of Ad amine in the dispersion of PS particles, which was determined by omitting EDC during coupling (Table S2). Nevertheless, the Ad loading determined through NMR analysis shows significant differences between different concentrations of Ad used for modifying PS particles and should therefore be seen as relative loading rather than as an absolute value.

3.2. Flow Rate Variation. The immobilization of the micrometer-sized particles was tested under different flow conditions ranging from 0.125 to 200 $\mu\text{L}/\text{min}$. PS-Cy5.5-0.8Ad particles (red) were successfully captured on β -CD lines as observed in images i–iv of Figure 2a, confirming that microparticle immobilization is feasible under flow conditions. Selectivity of Ad binding was shown by mixing Cy3-stained PS particles (PS-Cy3, yellow) without Ad [Figure 2a (v–viii)]. A reference surface was created by using μCP glycine, instead of β -CD, which confirmed that the immobilization of Ad-functionalized particles on β -CD-functionalized surfaces was the result of specific host–guest interactions (Figure S8; 5 $\mu\text{L}/\text{min}$ for 1 h).

Rinsing of the functionalized glass surfaces with DI water did not specifically remove immobilized particles, indicating strong binding interactions. Patterned binding of Ad-modified PS particles to the β -CD-modified glass surface confirms that the binding affinity is high enough to overcome the drag forces acting on the particles (see eq S1 and Table S3); the drag force acting on a microparticle for all flow rates is approximately 10^5 times lower than the binding strength of an individual Ad- β -CD host–guest complex (10^{-11} N).³⁵ However, this value for

Ad- β -CD binding strength is based on ideal conditions, not considering kinetic and concentration effects which are also important for binding affinity and particle immobilization. Therefore, it is still necessary to have multiple Ad- β -CD bonds for keeping particles immobilized on the surfaces during flow.

The influence of the flow rate on particle capturing was studied by varying the flow rate from 0.125 to 200 $\mu\text{L}/\text{min}$. Subsequently, the different flow rates were compared both on the density of captured particles and on specificity (Figures 2 and S9). The values for particle binding density and specificity of PS-Cy5.5-0.8Ad particles for the printed β -CD lines on the glass surface were calculated and plotted in Figure 2b,c. Looking at the particle binding density graph in Figure 2b and microscope images [Figure 2a (i–iv)], increasing the flow rate from 2.5 $\mu\text{L}/\text{min}$ until 200 $\mu\text{L}/\text{min}$ resulted in a decrease of immobilized particles from 3 to 0.5 PS-Cy5.5-0.8Ad particles/ $10^2 \mu\text{m}$ on β -CD. This finding is in line with the literature as particle deposition increases with lower flow rates.³⁶

Another important factor for assessing the immobilization of particles to modified surfaces is the particle binding specificity. The particle binding specificity, in this case, measures how well PS-Cy5.5-0.8Ad particles bind specifically to the patterns of β -CD compared to the aspecific binding to PEG backfilling and is plotted in (Figure 2c). From a flow rate of 2.5 $\mu\text{L}/\text{min}$ and above, samples have a binding specificity of $\geq 80\%$ for β -CD lines and with flow rates from 5 $\mu\text{L}/\text{min}$ and above, samples have the highest specificities above 90%. Using a flow rate of 0.125 and 0.25 $\mu\text{L}/\text{min}$ resulted in a lower binding specificity most significantly compared to the other flow rates, which is

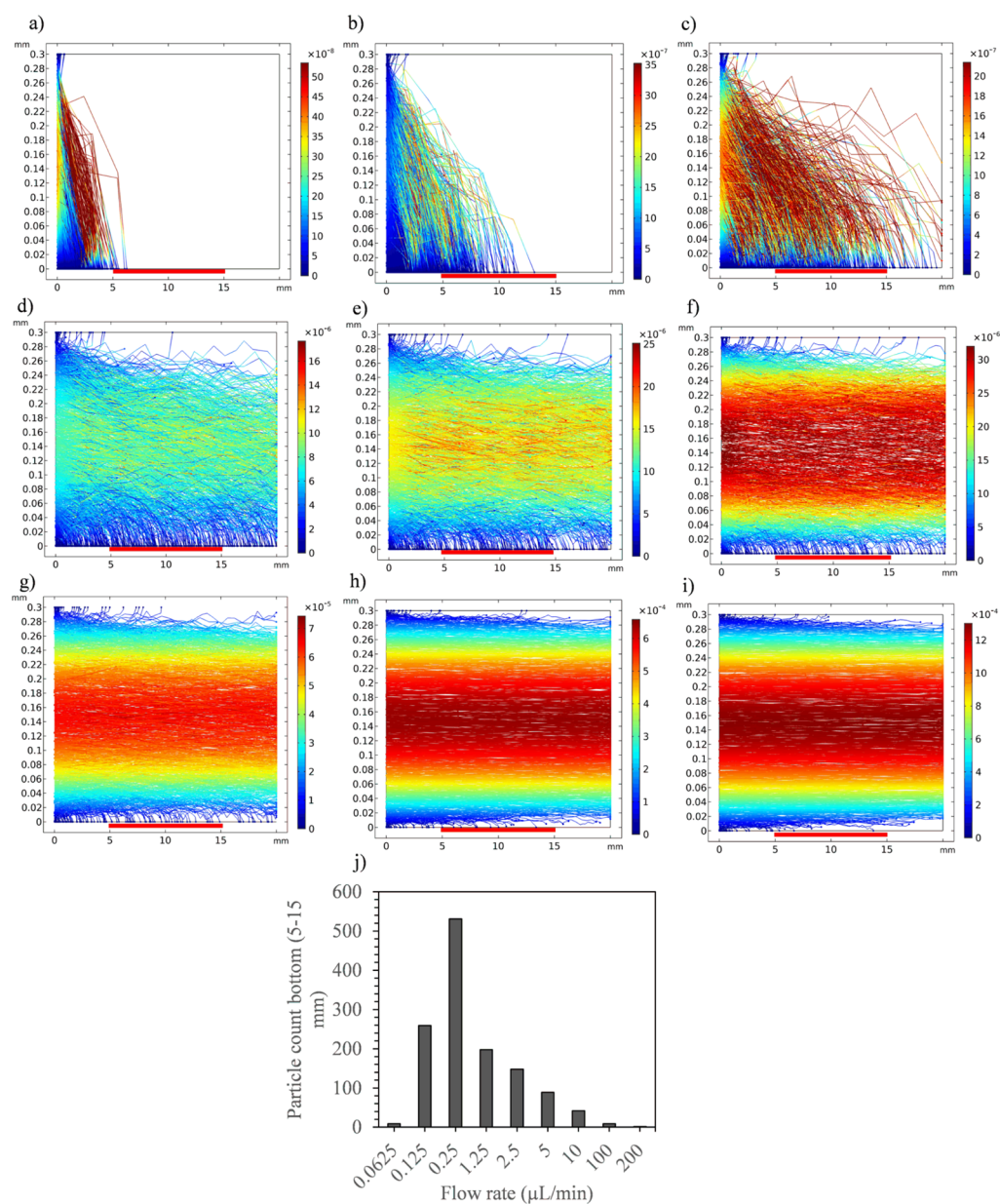


Figure 3. Consol particle tracing data of flow rates (a) 0.0625, (b) 0.125, (c) 0.25, (d) 1.25, (e) 2.5, (f) 5, (g) 10, (h) 100, and (i) 200 $\mu\text{L}/\text{min}$. The red line marks the area that was focused on for particle counting. The scale on the right side of each image for (a–i) shows the particle velocity in m/s. The particle size is scaled up for the viewing purpose. Both the bottom and top channel walls have stick conditions. (j) The graph showing the amount of particles stuck on the bottom channel wall from Consol simulation data vs flow rate used. The total amount of particles was 1480 in each simulation.

mostly because of the lower particle binding density. The amount of particles captured on the functionalized surfaces at flow rates from 10 $\mu\text{L}/\text{min}$ and above is considerably lower than that with 2.5 and 5 $\mu\text{L}/\text{min}$ flow rates (Figure 2b). Thus, a flow rate of 5 $\mu\text{L}/\text{min}$ for specific immobilization of these particles is most desirable, considering the particle binding density and specificity.

Surprisingly, when we carried out particle-capturing experiments at extremely low flow rates of 0.125 and 0.25 $\mu\text{L}/\text{min}$, almost no particles were bound to the printed β -CD surface. Consol particle flow simulations were carried out to investigate the change in particle binding to the β -CD-modified surface with flow rates. These calculations were made using a 2D flow cell geometry of 20 mm in length and 0.3 mm in height that represented the conditions in the Micronit flow

channel, 1 μm sized particles, similar flow rates, and stick conditions for both the bottom and top channel walls (Figure S3c). After carrying out simulations at different flow rates, particles were counted over the center of the bottom channel wall from 5 to 15 mm for each simulation, which is approximately where the glass surface in the practical experiments was patterned with β -CD through μCP . Indeed, a similar trend in particle binding density to the practical flow experiments was noticed in the Consol particle tracing data, when we focused on this area (Figure 3a–i), marked with a red line. It is also clear that the flow profile of trajectory graphs (a–d) (0.0625–1.25 $\mu\text{L}/\text{min}$ flow rate) is mostly based on diffusion and settling of particles, while in trajectory graphs (e,f) (2.5–200 $\mu\text{L}/\text{min}$ flow rate), a laminar flow profile is observed (Figure 3). In trajectory graphs (a) and (b) from

Figure 3, the particles stuck to the marked area on the bottom channel wall decreases dramatically because particles settle before they reach the designated area. The trend seen in the graph in Figure 3j correlates well with the experimental findings for the practical experiments in Figure 2. Therefore, a decrease is observed in particle binding density because of the particle settling before reaching the functionalized area with β -CD patterns in the middle of the channel. This was confirmed by carrying out a flow experiment at 0.125 $\mu\text{L}/\text{min}$ with only the PS-Cy3 particle on PEG-functionalized glass surfaces, which shows that most particles are situated in the inlet side of the flow channel after flow incubation (Figure S10).

Adversely, when increasing the flow rate within the laminar flow regime (between flow rates of 2.5 and 200 $\mu\text{L}/\text{min}$), the particle binding density also decreases within the practical experiments and simulation because the effect of gravity and diffusion is low. The effect of diffusion can be explained using the Péclet (Pe) number, which describes the effect of flow advection compared to that of particle diffusion. As mentioned above, we assume the laminar flow within the microfluidic channel at flow rates 2.5–200 $\mu\text{L}/\text{min}$, which means that the particle velocity decreases close to the channel walls (eq S2, Table S4). When the advection, that is, flow rate, increases and Pe numbers increase far above 1, particle diffusion can be seen as negligible. In Table S4, the Pe numbers were calculated for the different flow velocities of the particles that are 1 μm above the channel wall using eqs S3 and S4. For flow rates of 100 and 200 $\mu\text{L}/\text{min}$, the Pe numbers were considerably higher than 1, which explains the small difference in particle binding density. This is caused by a limitation in the amount of particles that can reach the bottom channel through diffusion or settling, while at flow rates from 2.5 to 10 $\mu\text{L}/\text{min}$, particle diffusion to the channel wall is possible from a larger distance (Figures S11 and S12). Therefore, there is a specific range of flow rates in which the increased effect of diffusion combined with advection allows for more Ad-functionalized PS particles to come in contact with the area patterned with β -CD and thus be immobilized.

For nonfunctionalized PS-Cy3 particles, significantly lower binding, ranging from 0.008 to 0.04 particles per 100 μm^2 (for flow rates 2.5–200 $\mu\text{L}/\text{min}$), was observed (Figure S13). The amount of PS-Cy3 particles, however, increases when higher amounts PS-Cy5.5-Ad particles were immobilized on the surface, which could be caused by aggregation of PS-Cy3 particles with PS-Cy5.5-Ad particles. An experiment with only PS-Cy3 particles carried out as a control at 5 $\mu\text{L}/\text{min}$ flow showed that almost no particles were bound to the glass surface (Figure S14).

To study the effect of particle settling on PS-Cy5.5-0.8Ad particle binding to the functionalized surface, an upside down flow experiment at 2.5 and 5 $\mu\text{L}/\text{min}$ was carried out by turning the flow cell holder upside down (Figure 4). These flow rates were chosen because the transition to laminar flow occurs at 2.5 and 5 $\mu\text{L}/\text{min}$, according to the particle trajectories in Figure 3. As observed in the microscopic images (Figure 4a), PS particle binding to β -CD patterns is still possible in upside down flow situations and was selective for PS-Cy5.5-0.8Ad particles. Compared to the upright flow experiment (Figure 2b), binding to the surface was \sim six times lower for 2.5 $\mu\text{L}/\text{min}$ at 0.4 particles per 100 μm^2 and \sim three times lower for 5 $\mu\text{L}/\text{min}$ at 0.8 particles per 100 μm^2 on β -CD patterns (Figure 4b). Therefore, particle settling has a significant effect in improving the contact of the PS particles

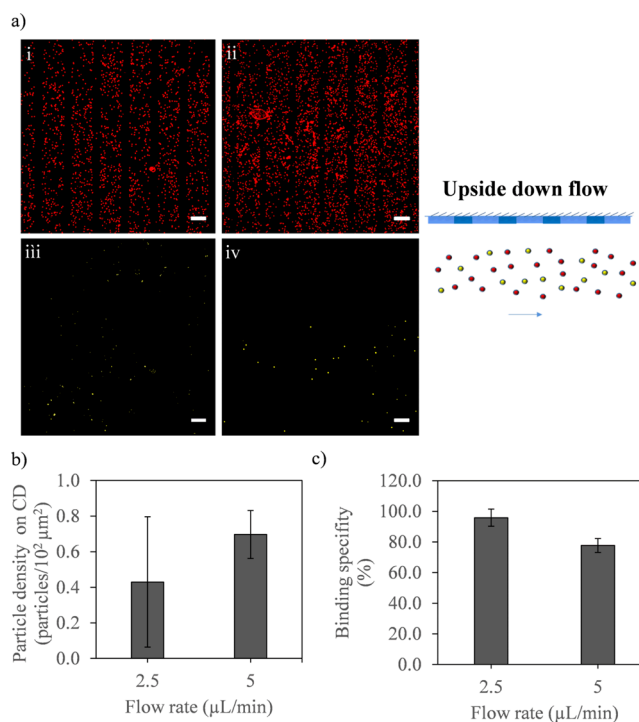


Figure 4. (a) Fluorescence microscope images of equimolar ratios of PS-Cy5.5-0.8Ad (i,ii) and PS-Cy3 particles (iii,iv) bound to β -CD-patterned glass surfaces after upside down flow incubation at 2.5 $\mu\text{L}/\text{min}$ (i,iii) and 5 $\mu\text{L}/\text{min}$ (ii,iv). The patterns are oriented perpendicular to the flow direction. The top images are captured with a Cy5 filter and the bottom images with a RHOD filter. Scale bars are 100 μm . (b) Graph showing particle density vs flow rate for upside down flow on β -CD patterns. (c) Graph showing binding specificity vs flow rate for upside down flow on β -CD patterns.

with the bottom channel wall. Nevertheless, PS-Cy5.5-0.8Ad particle binding to β -CD patterns is still feasible and specific through host–guest interactions without the aid of particle settling (Figure 4c).

3.3. Ad Loading Effect on PS Particle Binding. The PS-Ad samples with different surface coverages of Ad were made to flow over the β -CD glass surfaces and compared (Figure 5). At a flow rate of 5 $\mu\text{L}/\text{min}$, a clear increase in the particle density is observed for PS particles with higher Ad surface coverage and 0.15 Ad-loaded PS-Cy5.5 particles obtain a clear lower particle surface density (0.4 particles/ $100 \mu\text{m}^2 \beta$ -CD) than 0.3 and 0.8 Ad-loaded PS particles (1 and 2 particles/ $100 \mu\text{m}^2$, Figure 5a,b). An increase in the negative control PS-Cy3 particle density on β -CD is also seen with higher Ad loading of PS-Cy5.5-Ad (Figure S9). However, the PS-Cy3 particle density is still approximately 100 times lower than PS-Cy5.5-Ad density on cyclodextrin. PS-Cy5.5-Ad particle binding was very specific in all cases for β -CD patterns.

To shed light on the amount of Ad and β -CD pairs that are interacting to immobilize one Ad-functionalized PS particle, the accessible contact area of PS and β -CD was calculated to be ca. 2000 nm^2 , when a PS particle touches the glass surface (based on an Ad-NH₂ linker length of 0.6 nm). Assuming the Ad loading previously determined, the amount of Ad moieties present on the PS particle surface within the 2000 nm^2 contact area is approximately 2000 for PS-Cy5.5-0.15Ad, 4000 for PS-Cy5.5-0.3Ad, and 12 000 for PS-Cy5.5-0.8Ad. When assuming a β -CD surface density of 6×10^{-11} mol/ cm^2 on glass from the literature,²⁵ ca. 800 β -CD units are present in 2000 nm^2 on

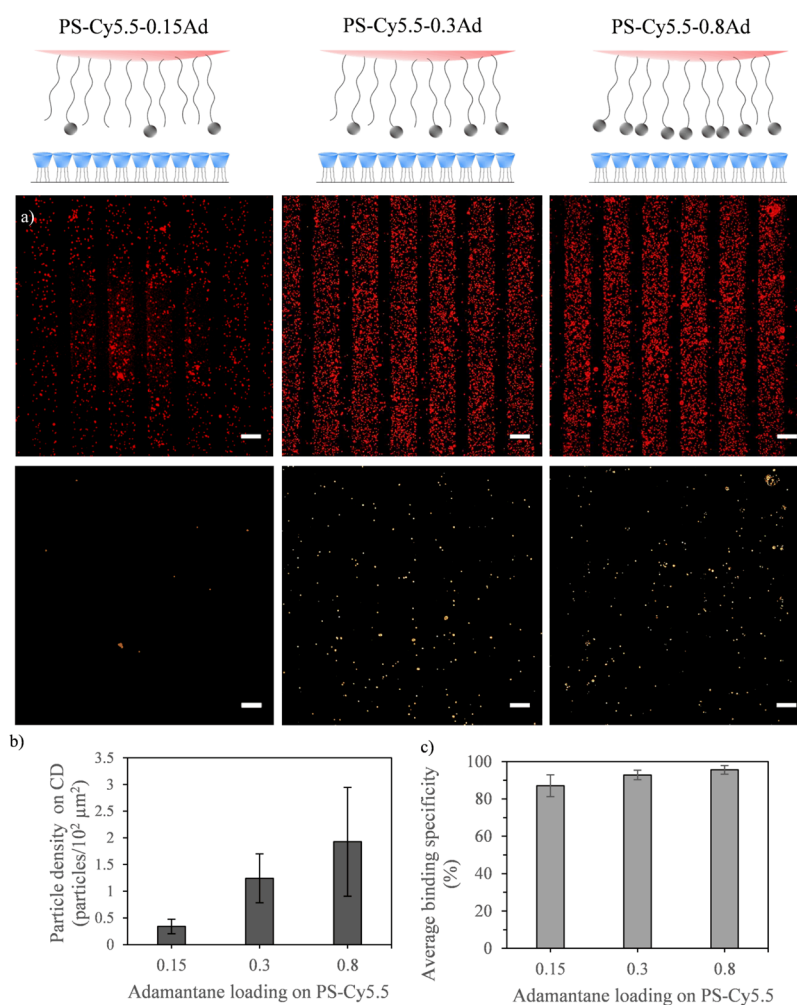


Figure 5. (a) Fluorescence microscope images of PS particles adhered to β -CD lines with different Ad loading on PS-Cy5.5-Ad particles of 0.15, 0.3, and 0.8 at a flow rate of $5 \mu\text{L}/\text{min}$. The patterns are oriented perpendicular to the flow direction. The Cy5 filter (red) shows PS-Cy5.5-Ad particles and the RHOD filter (yellow) shows PS-Cy3 particles. Scale bar is $100 \mu\text{m}$. (b) Graph showing particle density on β -CD vs Ad loading on the PS-Cy5.5 particle surface. (c) Graph showing binding specificity for β -CD patterns vs Ad loading on the PS-Cy5.5 particle surface.

glass. Interestingly, β -CD-Ad couples are therefore limited by the number of β -CD molecules rather than that of Ad. However, as mentioned before, in the characterization of the PS particles, actual Ad loading on the PS surface is most likely lower than the amounts calculated via NMR analysis. More importantly, the surface roughness of PS particles and glass can also reduce the amount of accessible Ad and β -CD molecules for host–guest interactions. Furthermore, the binding affinity is also governed by concentration gradients within a solution and kinetic effects, which increases the complexity in determining the amount of interactions required for microparticle immobilization to a surface. Therefore, we argue that these experimental findings and analyses show that determining the amount of interactions required for microparticle immobilization is not straightforward and requires further research. Nevertheless, these results do show that changing the relative amount of targeting molecules on the microparticle surface, thereby tuning the multivalency, plays an important role for increasing microparticle immobilization on functionalized surfaces.

3.4. Reversibility and Reusability of β -CD Glass Surfaces. The reversible nature of particle immobilization mediated by host–guest interactions was tested by removal of particles and re-addition of “new” particles (Figure 6). The

addition of the PS particle mix (PS-Cy5.5-0.8Ad and PS-Cy3) at $5 \mu\text{L}/\text{min}$ was carried out over the β -CD surfaces as before, and the surface was analyzed on the microscope. Rinsing with EtOH was attempted to diminish the hydrophobic interaction between β -CD and Ad.³⁷ In addition, rinsing with a concentrated solution of β -CD was performed to compete in the host–guest interaction.³² Unfortunately, both approaches did not result in significant release of the multivalently bound microparticles. Next, a more rigorous ultrasonic treatment in EtOH and subsequently water was applied. It is observed in Figure 6a that complete removal of PS particles was achieved and the glass surface is still functional for the subsequent particle immobilization experiment. Quantitative analysis for two particle immobilization experiments shows that two times less PS-Cy5.5-Ad particles are immobilized the second time (Figure 6b). This could be due to loss of β -CD functionality through ultrasonic treatment or because some EtOH is still present on the glass substrate that can diminish binding affinity of Ad for the β -CD cavity.

4. CONCLUSIONS

In summary, a chemically modified glass platform has been developed that can capture micrometer-sized particles on flow

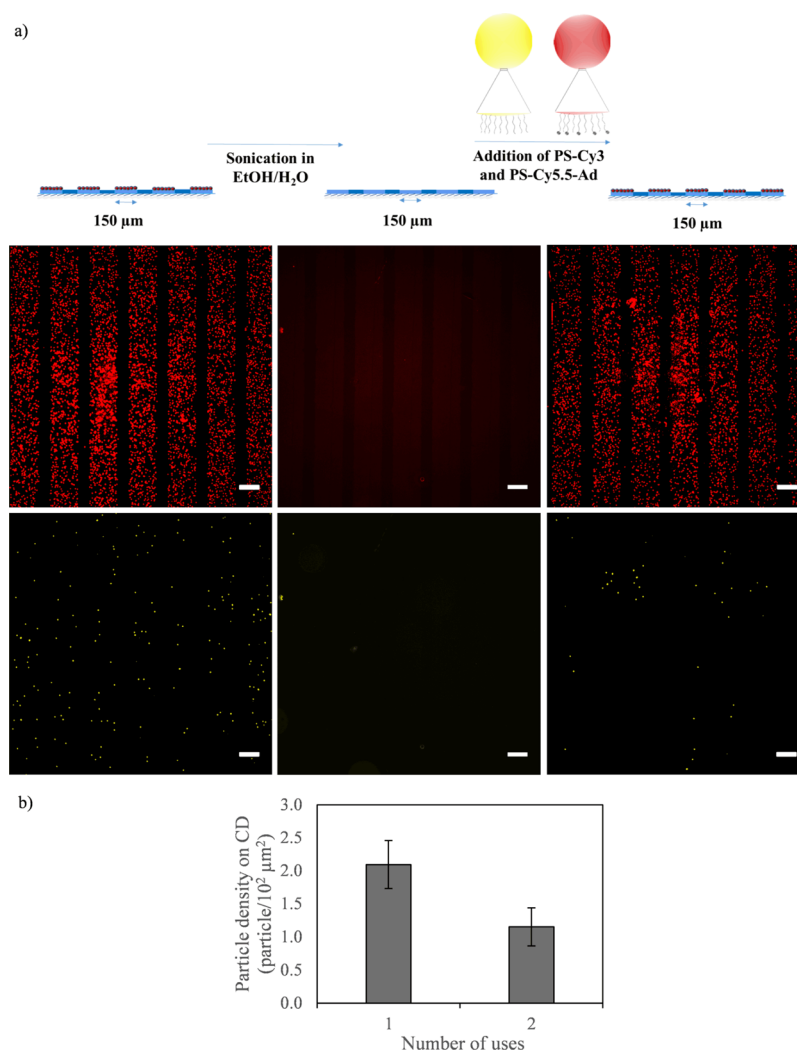


Figure 6. (a) Fluorescence microscope images of PS particles adhered to β -CD lines and subsequent removal and readdition of PS particles at a 5 $\mu\text{L}/\text{min}$ flow rate. Cy5 channels (red) show PS-Cy5.5-Ad particles and the RHOD channel (yellow) shows PS-Cy3 particles. (b) Particle density on β -CD after multiple uses.

in a recyclable manner. The capture of “large” particles, about 10^3 times larger than the host molecule β -CD, was possible through multivalent host–guest interactions between Ad and cyclodextrin. Immobilization of Ad-functionalized PS particles to β -CD-modified platforms was flow rate-dependent, with an optimal capturing density at 2.5–5 $\mu\text{L}/\text{min}$. Changing the degree of Ad functionalization on the PS particles influenced the degree of binding on the glass surfaces, underpinning the effect of multivalent host–guest interactions on particle binding. The modified glass platforms could also be recycled, highlighting the potential of using such systems in water purification setups. The depicted results of this model system show that host–guest interactions can bridge the gap between the nano- and microscale and also give insight into certain parameters and hurdles that are important to be taken into account for approaching the application of bacterial cell targeting in wastewater. Moreover, the experimental setup of this model system can be easily used for immobilization tests with different types of molecules or particles.

■ ASSOCIATED CONTENT

📄 Supporting Information

The Supporting Information is available free of charge on the ACS Publications website at DOI: 10.1021/acsami.9b11069.

Additional material on structure of dyes, characterization of PS particles (concentration determination, DLS, and conductivity), characterization of β -CD printed glass surfaces (fluorescence microscopy with Cy5-Ad₂), reverse conductometric titration of PS particles, comparison between flow cell channel dimension for experimental and Comsol simulation setup, NMR spectra of the supernatant from Ad-functionalized PS particles, calculation of Stokes drag force, Reynolds number, and Péclet number of particles at different flow rates, flow experiments of PS particle mix over glycine-printed flow cells, PS particle distribution after 20 h incubation with 0.25 $\mu\text{L}/\text{min}$ flow rate, PS-Cy3 particles over the β -CD-printed surface at 5 $\mu\text{L}/\text{min}$, all flow rate variation experiments for the PS particle mix, and quantitative analysis of PS-Cy3 particle binding to β -CD-printed surfaces (PDF)

AUTHOR INFORMATION

Corresponding Author

*E-mail: aldrik.velders@wur.nl.

ORCID

Fijfs W.B. van Leeuwen: 0000-0002-6844-4025

Aldrik H. Velders: 0000-0002-6925-854X

Author Contributions

The manuscript was written through contributions of all the authors. All the authors have given approval to the final version of the manuscript.

Notes

The authors declare no competing financial interest.

ACKNOWLEDGMENTS

This work was performed in the cooperation framework of Wetsus, European Centre of Excellence for Sustainable Water Technology (www.wetsus.eu). Wetsus is co-funded by the Dutch Ministry of Economic Affairs, the Ministry of Infrastructure and Environment, the Province of Fryslân, and the Northern Netherlands Provinces. The authors like to thank the members of the research theme Source Separated Sanitation for the shared knowledge and financial support. We acknowledge Mark Rood for preparing the Cy5-Ad₂ dye.

REFERENCES

(1) Mrksich, M.; Whitesides, G. M. Using Self-Assembled Monolayers to Understand the Interactions of Man-made Surfaces with Proteins and Cells. *Annu. Rev. Biophys. Biomol. Struct.* **1996**, *25*, 55–78.

(2) Anselme, K.; Davidson, P.; Popa, A. M.; Giazzon, M.; Liley, M.; Ploux, L. The Interaction of Cells and Bacteria with Surfaces Structured at the Nanometre Scale. *Acta Biomater.* **2010**, *6*, 3824–3846.

(3) Torkelson, A. A.; da Silva, A. K.; Love, D. C.; Kim, J. Y.; Alper, J. P.; Coox, B.; Dahm, J.; Kozodoy, P.; Maboudian, R.; Nelson, K. L. Investigation of Quaternary Ammonium Silane-Coated Sand Filter for the Removal of Bacteria and Viruses from Drinking Water. *J. Appl. Microbiol.* **2012**, *113*, 1196–1207.

(4) Shtarker-Sasi, A.; Castro-Sowinski, S.; Matan, O.; Kagan, T.; Nir, S.; Okon, Y.; Nasser, A. M. Removal of bacteria and *Cryptosporidium* from water by micelle-montmorillonite complexes. *Desalin. Water Treat.* **2013**, *51*, 7672–7680.

(5) Hagen, K. Removal of Particles, Bacteria and Parasites with Ultrafiltration for Drinking Water Treatment. *Desalination* **1998**, *119*, 85–91.

(6) MacRae, I. C.; Evans, S. K. Removal of Bacteria from Water by Adsorption to Magnetite. *Water Res.* **1984**, *18*, 1377–1380.

(7) Krasowska, A.; Sigler, K. How Microorganisms use Hydrophobicity and what does this mean for Human Needs? *Front. Cell. Infect. Microbiol.* **2014**, *4*, 112.

(8) Mrksich, M.; Dike, L. E.; Tien, J.; Ingber, D. E.; Whitesides, G. M. Using Microcontact Printing to Pattern the Attachment of Mammalian Cells to Self-Assembled Monolayers of Alkanethiolates on Transparent Films of Gold and Silver. *Exp. Cell Res.* **1997**, *235*, 305–313.

(9) Mrksich, M.; Chen, C. S.; Xia, Y.; Dike, L. E.; Ingber, D. E.; Whitesides, G. M. Controlling Cell Attachment on Contoured Surfaces with Self-Assembled Monolayers of Alkanethiolates on Gold. *Proc. Natl. Acad. Sci. U.S.A.* **1996**, *93*, 10775–10778.

(10) Kumar, A.; Biebuyck, H. A.; Whitesides, G. M. Patterning Self-Assembled Monolayers: Applications in Materials Science. *Langmuir* **1994**, *10*, 1498–1511.

(11) Ostuni, E.; Yan, L.; Whitesides, G. M. The Interaction of Proteins and Cells with Self-Assembled Monolayers of Alkanethiolates on Gold and Silver. *Colloids Surf., B* **1999**, *15*, 3–30.

(12) Kumar, A.; Whitesides, G. M. Patterned Condensation Figures as Optical Diffraction Gratings. *Science* **1994**, *263*, 60.

(13) Xia, Y.; Whitesides, G. M. Soft Lithography. *Angew. Chem., Int. Ed.* **1998**, *37*, 550–575.

(14) Sankaran, S.; van Weerd, J.; Voskuhl, J.; Karperien, M.; Jonkheijm, P. Photoresponsive Cucurbit[8]uril-Mediated Adhesion of Bacteria on Supported Lipid Bilayers. *Small* **2015**, *11*, 6187–6196.

(15) Sankaran, S.; Kiren, M. C.; Jonkheijm, P. Incorporating Bacteria as a Living Component in Supramolecular Self-Assembled Monolayers through Dynamic Nanoscale Interactions. *ACS Nano* **2015**, *9*, 3579–3586.

(16) Di Iorio, D.; Verheijden, M. L.; van der Vries, E.; Jonkheijm, P.; Huskens, J. Weak Multivalent Binding of Influenza Hemagglutinin Nanoparticles at a Sialoglycan-Functionalized Supported Lipid Bilayer. *ACS Nano* **2019**, *13*, 3413–3423.

(17) Szejtli, J. Introduction and General Overview of Cyclodextrin Chemistry. *Chem. Rev.* **1998**, *98*, 1743–1754.

(18) Loftsson, T.; Brewster, M. E. Pharmaceutical Applications of Cyclodextrins. 1. Drug Solubilization and Stabilization. *J. Pharm. Sci.* **1996**, *85*, 1017–1025.

(19) Park, C.; Kim, H.; Kim, S.; Kim, C. Enzyme Responsive Nanocontainers with Cyclodextrin Gatekeepers and Synergistic Effects in Release of Guests. *J. Am. Chem. Soc.* **2009**, *131*, 16614–16615.

(20) Onclin, S.; Mulder, A.; Huskens, J.; Ravoo, B. J.; Reinhoudt, D. N. Molecular Printboards: Monolayers of β -Cyclodextrins on Silicon Oxide Surfaces. *Langmuir* **2004**, *20*, 5460–5466.

(21) Ludden, M. J. W.; Reinhoudt, D. N.; Huskens, J. Molecular Printboards: Versatile Platforms for the Creation and Positioning of Supramolecular Assemblies and Materials. *Chem. Soc. Rev.* **2006**, *35*, 1122–1134.

(22) Gonzalez-Campo, A.; Hsu, S. H.; Puig, L.; Huskens, J.; Reinhoudt, D. N.; Velders, A. H. Orthogonal Covalent and Noncovalent Functionalization of Cyclodextrin-Alkyne Patterned Surfaces. *J. Am. Chem. Soc.* **2010**, *132*, 11434–11436.

(23) Krieg, E.; Bastings, M. M. C.; Besenius, P.; Rybtchinski, B. Supramolecular Polymers in Aqueous Media. *Chem. Rev.* **2016**, *116*, 2414–2477.

(24) de laRica, R.; Fratila, R. M.; Szarpak, A.; Huskens, J.; Velders, A. H. Multivalent Nanoparticle Networks as Ultrasensitive Enzyme Sensors. *Angew. Chem., Int. Ed.* **2011**, *50*, 5704–5707.

(25) Mahalingam, V.; Onclin, S.; Péter, M.; Ravoo, B. J.; Huskens, J.; Reinhoudt, D. N. Directed Self-Assembly of Functionalized Silica Nanoparticles on Molecular Printboards through Multivalent Supramolecular Interactions. *Langmuir* **2004**, *20*, 11756–11762.

(26) Dorokhin, D.; Hsu, S.-H.; Tomczak, N.; Reinhoudt, D. N.; Huskens, J.; Velders, A. H.; Vancso, G. J. Fabrication and Luminescence of Designer Surface Patterns with β -Cyclodextrin Functionalized Quantum Dots via Multivalent Supramolecular Coupling. *ACS Nano* **2010**, *4*, 137–142.

(27) Harada, A.; Kobayashi, R.; Takashima, Y.; Hashidzume, A.; Yamaguchi, H. Macroscopic self-assembly through molecular recognition. *Nat. Chem.* **2010**, *3*, 34.

(28) Appel, J.; Akerboom, S.; Fokkink, R. G.; Sprakel, J. Facile One-Step Synthesis of Monodisperse Micron-Sized Latex Particles with Highly Carboxylated Surfaces. *Macromol. Rapid Commun.* **2013**, *34*, 1284–1288.

(29) Bangs Laboratories, Inc. *Covalent Coupling, TechNote*, 2002; Vol. 20, pp 1–9.

(30) Hen, J. Determination of surface carbonyl groups in styrene/itaconic acid copolymer latexes. *J. Colloid Interface Sci.* **1974**, *49*, 425–432.

(31) Rood, M. T. M.; Spa, S. J.; Welling, M. M.; ten Hove, J. B.; van Willigen, D. M.; Buckle, T.; Velders, A. H.; van Leeuwen, F. W. B. Obtaining Control of Cell Surface Functionalizations via Pre-Targeting and Supramolecular Host-Guest Interactions. *Sci. Rep.* **2017**, *7*, 39908.

(32) Mulder, A.; Onclin, S.; Péter, M.; Hoogenboom, J. P.; Beijleveld, H.; ter Maat, J.; García-Parajó, M. F.; Ravoo, B. J.

Huskens, J.; van Hulst, N. F.; Reinhoudt, D. N. Molecular Printboards on Silicon Oxide: Lithographic Patterning of Cyclodextrin Monolayers with Multivalent, Fluorescent Guest Molecules. *Small* **2005**, *1*, 242–253.

(33) Carrazana, J.; Jover, A.; Mejjide, F.; Soto, V. H.; Vázquez Tato, J. Complexation of Adamantyl Compounds by β -Cyclodextrin and Monoaminoderivatives. *J. Phys. Chem. B* **2005**, *109*, 9719–9726.

(34) Schaefer, D. M.; Carpenter, M.; Gady, B.; Reifenberger, R.; Demejo, L. P.; Rimai, D. S. Surface roughness and its influence on particle adhesion using atomic force techniques. *J. Adhes. Sci. Technol.* **1995**, *9*, 1049–1062.

(35) Auletta, T.; de Jong, M. R.; Mulder, A.; van Veggel, F. C.; Huskens, J.; Reinhoudt, D. N.; Zou, S.; Zapotoczny, S.; Schönherr, H.; Vancso, G. J. β -Cyclodextrin Host-Guest Complexes Probed under Thermodynamic Equilibrium: Thermodynamics and AFM Force Spectroscopy. *J. Am. Chem. Soc.* **2004**, *126*, 1577–1584.

(36) Kuipers, R.; Saidi, M. H. Transportation and Settling Distribution of Microparticles in Low-Reynolds-Number Poiseuille Flow in Microchannel. *J. Dispersion Sci. Technol.* **2015**, *37*, 582–594.

(37) Harrison, J. C.; Eftink, M. R. Cyclodextrin-adamantanecarboxylate inclusion complexes: A model system for the hydrophobic effect. *Biopolymers* **1982**, *21*, 1153–1166.